

Optimization of metro vertical alignment for minimized construction costs and traction energy

Wang, Qian; Bai, Yun; Chen, Yao; Fu, Qian; Schonfeld, Paul

DOI:

[10.1016/j.tust.2022.104722](https://doi.org/10.1016/j.tust.2022.104722)

License:

Creative Commons: Attribution-NonCommercial-NoDerivs (CC BY-NC-ND)

Document Version

Peer reviewed version

Citation for published version (Harvard):

Wang, Q, Bai, Y, Chen, Y, Fu, Q & Schonfeld, P 2022, 'Optimization of metro vertical alignment for minimized construction costs and traction energy: a dynamic programming approach', *Tunnelling and Underground Space Technology*, vol. 129, 104722. <https://doi.org/10.1016/j.tust.2022.104722>

[Link to publication on Research at Birmingham portal](#)

General rights

Unless a licence is specified above, all rights (including copyright and moral rights) in this document are retained by the authors and/or the copyright holders. The express permission of the copyright holder must be obtained for any use of this material other than for purposes permitted by law.

- Users may freely distribute the URL that is used to identify this publication.
- Users may download and/or print one copy of the publication from the University of Birmingham research portal for the purpose of private study or non-commercial research.
- User may use extracts from the document in line with the concept of 'fair dealing' under the Copyright, Designs and Patents Act 1988 (?)
- Users may not further distribute the material nor use it for the purposes of commercial gain.

Where a licence is displayed above, please note the terms and conditions of the licence govern your use of this document.

When citing, please reference the published version.

Take down policy

While the University of Birmingham exercises care and attention in making items available there are rare occasions when an item has been uploaded in error or has been deemed to be commercially or otherwise sensitive.

If you believe that this is the case for this document, please contact UBIRA@lists.bham.ac.uk providing details and we will remove access to the work immediately and investigate.

1 Optimization of Metro Vertical Alignment for Minimized Construction Costs 2 and Traction Energy: A Dynamic Programming Approach

3 Qian Wang ^a, Yun Bai ^{a,*}, Yao Chen ^{a,*}, Qian Fu ^b, Paul Schonfeld ^c

4 ^aKey Laboratory of Transport Industry of Big Data Application Technologies for Comprehensive
5 Transport, Beijing Jiaotong University, Beijing, 100044, China

6 * E-mail: chenyaoyao@bjtu.edu.cn (corresponding author), Phone: +86 13120385660
7 yunbai@bjtu.edu.cn (corresponding author), Phone: +86 13401011428

8 ^b Birmingham Centre for Railway Research and Education, School of Engineering, University of
9 Birmingham, Birmingham B15 2TT, UK

10 ^c Department of Civil and Environmental Engineering, University of Maryland, College Park, MD
11 20742, United States

12
13 **Abstract:** Vertical alignment significantly affects the construction costs and train traction energy
14 use of a metro system. Existing studies on this subject mostly optimized the vertical alignment while
15 considering train traction energy consumption or construction costs only. There is still a lack of
16 efficient approach for the vertical alignment optimization problem which considers both
17 construction costs and traction energy consumption. To this end, this paper proposes a two-stage
18 optimization program involving both the design of metro vertical alignment and train speed profile,
19 with the objective of minimizing the total costs of construction and train traction energy. An iterative
20 approach is proposed for solving the two-stage program, in which a dynamic programming (DP)
21 algorithm with a backward search method is designed to seek an optimal vertical alignment given
22 an energy-efficient train speed profile. The model and algorithm approach are tested on real-world
23 case studies on the Line 14 of Guangzhou Metro in China. The results show that compared with the
24 existing heuristic algorithms, the DP approach performs better in computation time and solution
25 quality. Moreover, the optimized vertical alignments outperform that designed by experienced
26 designers in terms of total costs of construction and traction energy consumption, with an average
27 savings rate of 6.0%.

28 **Keywords:** Metro line; Vertical alignment; Construction cost; Train movement; Dynamic
29 programming

30 1 Introduction

31 1.1 Problem statement

32 Recent decades have seen continual and rapid development of metro systems in many countries

33 (especially in many large cities in China). A constantly expanding metro network incurs
34 considerable expenditure on construction and operation, including energy consumption. Since 2010,
35 for example, the total investment in the construction of the Guangzhou Metro – one of China’s
36 busiest metro systems – has reached 161.8 billion Chinese Yuan (Guangzhou Statistics Bureau,
37 2020), and its annual energy consumption has increased by about 1.2 billion kWh in a decade.
38 Despite numerous studies that have been conducted on various aspects of total costs reduction for a
39 metro system, there is still room for better solutions.

40 The design of metro alignment is one of the technical aspects that affect the total costs for a
41 metro system. It is aimed at finding an economical route of metro tracks between an origin and a
42 terminal, given local soil conditions, socio-economic factors, and environmental factors such as air
43 pollution and noise around the transit service area (Shafahi and Shahbazi, 2012, Li et al., 2016, and
44 Ghoreishi et al., 2019). The design includes aspects of both horizontal and vertical track alignments,
45 which are usually implemented in sequence. First, the design of horizontal alignment mostly
46 determines locations of metro stations, and tangents, horizontal, and transition curves. On that basis,
47 the design of vertical alignment determines the length and gradient of a slope and vertical curves
48 that connect two adjacent slopes.

49 This paper deals with modeling and optimization of a metro line’s vertical alignment. The
50 vertical alignment, on the one hand, is closely related to the construction of underground
51 infrastructure including line foundations, stations, tunnels, bridges, rights of way, utilities, and so
52 forth (Jha et al., 2007, Bababeik and Monajjem, 2012, Li et al., 2016), which rely on huge capital
53 investment. On the other hand, it has a significant impact on the running resistance of metro trains,
54 and hence on train traction energy consumption (Duarte and Sotomayor, 1999). The traction energy
55 consumption of a metro train refers to the electrical energy consumed by the traction system on the
56 train for vehicle propulsion and on-board auxiliary equipment; it can account for approximately half
57 of the total energy consumption in a metro system. Therefore, finding the lowest possible sum of
58 construction and traction energy cost is important for the design of metro vertical alignment.

59 Metro vertical alignment optimization must adhere to geographical compliance requirements
60 and specific geometric constraints. For underground constructions such as a metro line, it is vital to
61 eliminate the risk of geological hazards (e.g., drift-sand and sludge layers) and bypass any existing
62 underground facilities (e.g., oil and gas pipelines). Besides, the vertical alignment of the metro line
63 must also satisfy specific geometric specifications, such as a maximum gradient and a minimum
64 sloped length, to ensure train running safety. Professional engineers may decide on a feasible

65 vertical alignment design from among a small number of candidates by using their hands-on
66 experience. In reality, however, there could be a potentially unlimited number of feasible schemes
67 of the vertical alignment, and the empirically-chosen one may not necessarily be optimal (Li et al.,
68 2016, Samanta and Jha, 2011).

69 **1.2 Literature review**

70 Researchers have devoted great efforts to the optimization of vertical alignment in the areas of
71 both highways and railways. The studies on the highway vertical alignment are mostly intended to
72 minimize construction costs and energy consumption. Easa (1988) obtained an optimized vertical
73 alignment scheme, which minimized the cost of earthwork and met the geometric specifications via
74 an enumeration method. Fwa et al., (2002) then used a genetic algorithm (GA) to minimize the
75 associated construction costs. Furthermore, Goktepe et al., (2005) proposed a dynamic
76 programming (DP) approach to find an optimal vertical alignment with a minimum construction
77 cost given a few design constraints; and later, Goktepe et al., (2009) developed a GA-based
78 constrained curve-fitting technique considering vague soil parameters as required by the design of
79 the highway vertical alignment. Hare et al. (2015) presented a mixed integer linear programming
80 model, which also aims to minimize the cost of earthwork. More recently, Vandanjon et al., (2019)
81 proposed a method that considered both construction costs and energy consumption.

82 For optimizing railway vertical alignments, Hoang et al. (1975) proposed a model to obtain the
83 optimal gradient and length of slopes of inter-station tracks among six types of vertical alignment.
84 Further, Lafortune and Polis (1983) applied an “interactive computer aided analysis and design”
85 technique to automatically produce energy-efficient vertical alignment, considering various design
86 criteria of a metro system. Kim and Schonfeld (1997) developed a model for analyzing the train
87 traction energy and travel time with different dipped vertical alignments designed for gravity-
88 assisted acceleration and braking. Duarte and Sotomayor (1999) proposed a Gradient-Restoration
89 method to determine the vertical alignment together with an optimal control policy of a train in
90 metro systems. Xin et al. (2014) developed a simulation-based approach to optimize the metro
91 vertical alignment within the station area for minimizing the traction energy consumption. Kim et
92 al. (2013) compared the train traction energy among three vertical alignments connecting rail transit
93 stations. Li et al. (2022) proposed a Gaussian pseudo-spectral method to find an optimal design of
94 metro vertical alignment focusing on both traction energy consumption and running time deviation.

95 Other studies on railway vertical alignment optimization focused on the construction costs and
96 the operating costs without considering the train traction energy. Bababeik and Monajjem (2012)

97 developed a standard GA in a continuous search space to minimize the total construction and
 98 operating costs. Li et al. (2016) proposed a bidirectional two-dimensional distance transform (DT)
 99 algorithm to optimize the railway alignments, considering the costs of various factors including
 100 construction, operation, right-of-way, and environment. To improve computational efficiency in the
 101 optimization process, Pu et al. (2019) proposed a sequential three-dimensional DT algorithm in
 102 mountainous regions. On that basis, Song et al. (2020) considered a parallel three-dimensional DT
 103 algorithm to further boost computational efficiency. Around the same time, Costa et al. (2017)
 104 proposed an optimization method for three-dimensional alignment of the underground tunnel, which
 105 considered uncertainties associated with geology and construction processes. Ghoreishi et al. (2019)
 106 proposed a particle swarm optimization (PSO) algorithm, with the support of a geographic
 107 information system for three-dimensional optimization of railway alignments.

108 More recent studies have focused on optimizing the vertical alignment by minimizing
 109 concurrently the construction costs and traction energy consumption. Lai and Schonfeld (2012)
 110 proposed a GA-based method to optimize the vertical track alignment of urban rail transit. Kim et
 111 al. (2019) proposed a GA combined with a simulation model to find solutions for railway vertical
 112 alignment and train operating speed. Zhang et al. (2021) formulated a model for the 3D railway
 113 alignment optimization problem, which was solved by a stepwise and hybrid particle swarm-genetic
 114 algorithm.

115 Table 1 Methods for railway vertical alignment optimization

| References | Construction costs | Traction energy consumption | Approaches |
|------------------------------|--------------------|-----------------------------|--------------------------|
| Hoang et al. (1975) | × | ✓ | Enumeration |
| Duarte and Sotomayor (1999) | × | ✓ | Gradient- Restoration |
| Fwa et al. (2002) | ✓ | × | GA |
| Bababeik and Monajjem (2012) | ✓ | × | GA |
| Lai and Schonfeld (2012) | ✓ | ✓ | GA |
| Li et al. (2016) | ✓ | × | 2D-DT |
| Kim et al. (2019) | ✓ | ✓ | GA |
| Pu et al. (2019) | ✓ | × | 3D-DT |
| Ghoreishi et al. (2019) | ✓ | × | PSO |

116
 117 Table 1 summarizes the methods used in the relevant studies of the railway vertical alignment
 118 design. Due to nonlinear constraints and very large solution space, most of the existing studies

119 employed heuristic algorithms to obtain a near-optimal solution. Heuristic algorithms have
120 randomness in problem solving process and cannot guarantee the stability of their final solutions.
121 Therefore, there is still no exact approach for tackling the vertical alignment optimization problem,
122 while considering both the construction costs and traction energy consumption.

123 **1.3 Aim and contributions of the study**

124 The study presented in this paper aims to develop a two-stage optimization program involving
125 both the design of metro vertical alignment and train speed profile, with the objective of minimizing
126 the total costs of construction and traction energy. The main contributions of this paper are as
127 follows:

- 128 1) Unlike most existing studies on vertical alignment design that only consider train traction
129 energy consumption or construction costs, this study minimizes the total of the two terms to
130 involve the impact of vertical alignment schemes on both metro construction and train
131 operation. To explicitly characterize the interaction between the vertical alignment and train
132 speed profile, this paper develops a two-stage program to integrate train speed profile
133 optimization into vertical alignment design, in which the first stage determines the vertical
134 alignment, and the second stage minimizes the train traction energy consumption by optimizing
135 train speed profile given every vertical alignment scheme.
- 136 2) We propose an iterative approach that combines a DP algorithm and a brute force (BF)
137 algorithm to solve the two-stage optimization program, in which a DP algorithm is designed to
138 optimize the vertical alignment given an energy-efficient train speed profile. A two-dimensional
139 grid system is built to transform the vertical alignment optimization problem into a multi-stage
140 decision problem and a backward search method is proposed to seek the best vertical alignment.
- 141 3) Based on real-world case studies, the proposed DP algorithm has a better performance than the
142 simulated annealing genetic algorithm (SA-GA) and PSO algorithm. Moreover, compared to
143 the vertical alignment designed by experienced designers, the vertical alignment designed with
144 the iterative approach can reduce the total costs of construction and traction energy consumption
145 by 6.0% on average.

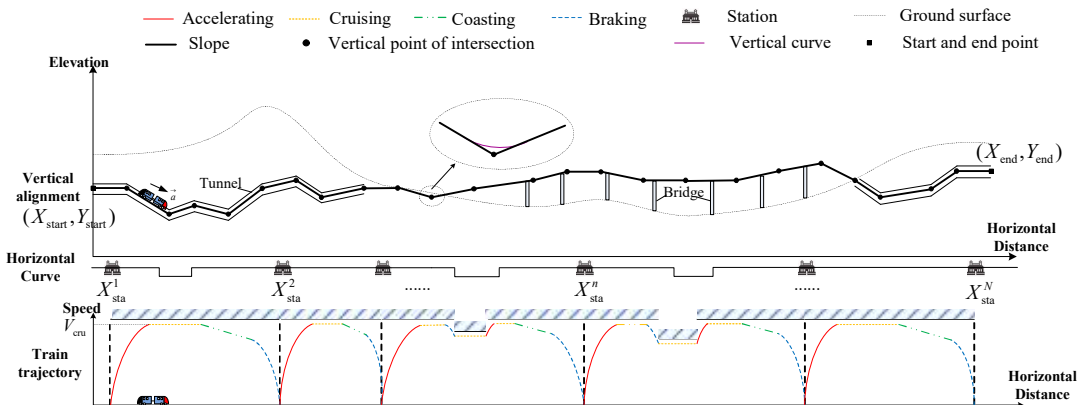
146 The rest of the paper is organized as follows. Section 2 describes the problem of designing
147 metro vertical alignment. Section 3 describes the two-stage optimization program. Then Section 4
148 describes the iterative approach for solving the two-stage optimization program. Section 5
149 demonstrates the proposed model and algorithm approach with case studies conducted on the Line
150 14 of Guangzhou Metro in China. Finally, Section 6 concludes the paper.

151 **2 Problem description**

152 This paper focuses on the vertical alignment design of a double-track metro line for a fixed
 153 horizontal alignment. As illustrated in Fig. 1, the horizontal locations of the metro stations and the
 154 horizontal curves between stations are pre-determined. The total number of metro stations is denoted
 155 by N , and $X_{sta}^n, n \in \{1, 2, \dots, N\}$ denotes the horizontal location of stations. The geographical features
 156 of the metro track, such as ground surface and locations of underground facilities, are known from
 157 field surveys.

158 The design of track vertical alignment between a given pair of start and end stations involves
 159 the determination of a number of parameters, such as lengths and gradients of slopes and vertical
 160 curves that connect two adjacent slopes. As shown in Fig. 1, let (X_{start}, Y_{start}) and (X_{end}, Y_{end}) denote
 161 the geographical coordinates of a start point and an end point, respectively. Two adjacent slopes are
 162 connected at a vertical point of intersection (VPI); a sequence of VPIs can determine the length and
 163 gradient of the slopes. Let (X_k, Y_k) denote the geographical coordinates of the k^{th} VPI, where
 164 $k \in \{1, 2, \dots, K\}$, with K being the total number of VPIs along the metro track.

165



166
 167
 168

Fig. 1. The vertical alignment of a metro track.

169 Generally, the construction costs of a metro system include track cost C_{TRA} , earthwork cost
 170 C_{EAR} , bridge cost C_{BRI} , tunnel cost C_{TUN} , right-of-way cost C_{RIG} , and station cost C_{STA} .
 171 Specifically, the volume of cuts and fills, and the lengths of bridges and tunnels are related to the
 172 elevations of track alignment and ground surface. Besides, the area occupied by the stations and
 173 tracks is closely related to the elevation of the track alignment and to their horizontal locations,
 174 which affect the right-of-way cost and station cost. Therefore, the proper design of the vertical
 175 alignment can reduce construction costs.

176 Train traction energy consumption is greatly affected by the slopes along the metro line. Due

177 to gravitational assistance, a downhill slope reduces the energy consumption of trains when they
178 accelerate or cruise. Conversely, an uphill slope reduces the braking energy dissipation needed to
179 decelerate trains. The traction energy consumption is an important factor in vertical alignment
180 design. However, the traction energy consumption is also determined by train speed profile. Given
181 a vertical alignment scheme, different train speed profiles can lead to various traction energy
182 consumption. The optimized train speed profile should be used to evaluate the traction energy
183 consumption. We assume that the train speed profile follows the control sequence of maximum
184 acceleration, cruising, coasting, and maximum braking, which is proved to be the most energy-
185 efficient train control strategy (Howlett, 1990; Howlett et al., 2009). With the energy-efficient train
186 control sequence, the train speed profile is optimized by determining the switching points from the
187 accelerating phase to the cruising phase and from the cruising phase to the coasting phase to
188 minimize traction energy consumption.

189 The metro vertical alignment design problem aims to optimize the geographic location of VPIs
190 under multiple constraints on geometry and geography with the fixed horizontal alignment. The
191 objective is to minimize the total costs of construction and traction energy consumption under the
192 optimized train speed profile.

193 **3 Model formulation**

194 In this section, we propose in detail an integrated two-stage optimization program that is used
195 to determine both metro vertical alignment and train speed profile. The first-stage program
196 optimizes metro vertical alignment by minimizing the total costs of construction and train traction
197 energy. The second-stage program minimizes the train traction energy consumption by optimizing
198 train speed profile given every vertical alignment scheme. The two-stage program is based on two
199 assumptions:

200 **Assumption 1.** The radius of a vertical curve is assumed constant (see also Li et al., 2013,
201 Song et al, 2022), as it usually remains unchanged once the design speed of the metro line is
202 determined (Code for Design of Metro, 2013).

203 **Assumption 2.** The reuse of train regenerative braking energy is not considered (see also Lai
204 and Schonfeld, 2012, Wang et al, 2021).

205 **3.1 Vertical alignment optimization**

206 **3.1.1 Decision variables**

207 The first-stage program is formulated as a vertical alignment optimization model. The core

208 decision variables of the first-stage model are the number of VPIs and the geographical coordinates
 209 of each VPI. The gradient and length of slopes are intermediate variables of the model. Let i_k denote
 210 the gradient, and l_k the length, of the k^{th} slope. They can be further represented, respectively, by
 211 Eqs. (1) and (2):

$$212 \quad i_k = \frac{Y_k - Y_{k-1}}{X_k - X_{k-1}}, \forall k \in \{1, 2, \dots, K\} \quad (1)$$

$$213 \quad l_k = X_k - X_{k-1}, \forall k \in \{1, 2, \dots, K\} \quad (2)$$

214 Moreover, the elevations of a metro track are also intermediate variables. We divide the metro
 215 track by distance intervals Δs . The set of geographical elevations of the metro track can be denoted
 216 by $\{h_{\text{tra}}^1, h_{\text{tra}}^2, \dots, h_{\text{tra}}^s, \dots, h_{\text{tra}}^K\}$, where h_{tra}^s denotes the track elevation at horizontal location s and it can
 217 be computed with Eq. (3) as follows:

$$218 \quad h_{\text{tra}}^s = i_k \cdot (s - X_k) + Y_k, \forall k \in \{1, 2, \dots, K\}, \text{ if } X_k \leq s < X_{k+1} \quad (3)$$

219 3.1.2 Objective function

220 To consider the life cycle of the metro line, the annual total costs of construction and train
 221 traction energy is set as the overall objective function of the first-stage model, which is expressed
 222 as:

$$223 \quad \min C_{\text{TOL}} = \mu \cdot C_{\text{CON}} + E(X_k, Y_k) \quad (4)$$

224 where C_{TOL} is the annual total costs; C_{CON} denotes the construction costs of the metro line. The
 225 ratio μ is the capital recovery factor, which is used to compute the annual construction costs. It is
 226 equal to $(1+i)^n i / [(1+i)^n - 1]$, where i denotes the interest rate per period and n represents the
 227 number of equal compounding periods in the entire economic life. $E(X_k, Y_k)$ is the second-stage
 228 objective function, which indicates the annual traction energy consumption associated with the first-
 229 stage decision variables (X_k, Y_k) .

230 The construction costs of the metro line include the track cost C_{TRA} , bridge cost C_{BRI} , tunnel
 231 cost C_{TUN} , earthwork cost C_{EAR} , right-of-way cost C_{RIG} , and station cost C_{STA} , as expressed in Eq.
 232 (5):

$$233 \quad C_{\text{CON}} = C_{\text{TRA}} + C_{\text{BRI}} + C_{\text{TUN}} + C_{\text{EAR}} + C_{\text{RIG}} + C_{\text{STA}} \quad (5)$$

234 According to Eq. (6), the track cost C_{TRA} is proportional to the total length and the unit track
 235 cost per meter, which is

$$236 \quad C_{\text{TRA}} = \sum_{k=1}^K c_{\text{tra}} \cdot l_k \quad (6)$$

237 where c_{tra} is the unit track cost per meter.

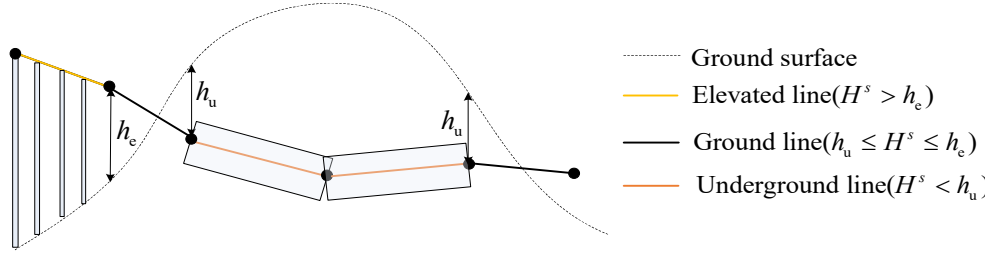


Fig. 3. The three types of metro line.

The earthwork cost, bridge cost and tunnel cost are related to the elevation difference between the metro track and the ground surface. Let h_{gro}^s denote the elevation of the ground surface at the horizontal location s . The elevation difference between the metro track and the ground surface is denoted by H^s , which is computed as:

$$H^s = h_{tra}^s - h_{gro}^s \quad (7)$$

Let h_{minb} and h_{mint} denote the minimum height of a bridge and the minimum depth of a tunnel, respectively. As shown in Fig. 3, firstly, when $H^s > h_{minb}$, the elevated metro line should be built on the bridges; secondly, when $-H^s > h_{mint}$, the metro line should be constructed in tunnels; thirdly, when $-h_{mint} \leq H^s \leq h_{minb}$, the metro line is constructed on the ground with cuts and fills. With the track elevations at different horizontal locations, the numbers of bridges and tunnels, which are denoted by n_{bri} and n_{tun} , respectively, can be derived.

The bridge cost C_{BRI} is related to the bridge height and length as well as the cost of bridge abutment, which is computed by Eq. (8) as:

$$C_{BRI} = \sum_i^{n_{bri}} \left[l_{bri}^i \cdot c_{bri}^i (H_{bri}^i) + \left\lfloor \frac{l_{bri}^i}{s_{maxb}} \right\rfloor \cdot c_{abu} \right] \quad (8)$$

where n_{bri} is the number of bridges, l_{bri}^i is the length of i^{th} bridge; H_{bri}^i is the height of i^{th} bridge (i.e., the elevation difference between the elevated track and ground surface), c_{bri}^i is the unit bridge cost per meter for the i^{th} bridge, which is a function of bridge height; c_{abu} denotes the cost of one bridge abutment; s_{maxb} represents the maximum bridge length; and the number of abutment is computed as $\left\lfloor l_{bri}^i / s_{maxb} \right\rfloor$.

The tunnel cost C_{TUN} is largely influenced by the tunnel length and the cost of tunnel portals. It is expressed as:

$$C_{TUN} = \sum_i^{n_{tun}} \left[l_{tun}^i \cdot c_{tun} + 2 \cdot c_{por} \right] \quad (9)$$

where n_{tun} is the number of tunnels, l_{tun}^i is the length of the i^{th} tunnel, c_{tun} is the unit tunnel cost per meter, c_{por} denotes the cost of one tunnel portal.

The volume of cuts and fills is influenced by the area of metro track occupied and the elevation

265 difference between the metro track and the ground surface, which can be computed with Eqs. (10)
 266 and (11) as follows:

$$267 \quad V_{\text{cut}} = \sum_{s=0}^S \Delta s \cdot D_w \cdot (h_{\text{gro}}^s - h_{\text{tra}}^s), \text{ if } 0 < h_{\text{tra}}^s - h_{\text{gro}}^s \leq h_{\text{minb}} \quad (10)$$

$$268 \quad V_{\text{fill}} = \sum_{s=0}^S \Delta s \cdot D_w \cdot (h_{\text{tra}}^s - h_{\text{gro}}^s), \text{ if } -h_{\text{mint}} \leq h_{\text{tra}}^s - h_{\text{gro}}^s < 0 \quad (11)$$

269 where V_{cut} and V_{fill} denote the volume of cuts and fills, respectively; and D_w represents the width
 270 of metro track alignment.

271 The earthwork cost C_{EAR} can be computed by summing up the product of the unit cost of cut
 272 and fill and the corresponding earthwork volume, which is represented by

$$273 \quad C_{\text{EAR}} = V_{\text{cut}} \cdot c_{\text{cut}} + V_{\text{fill}} \cdot c_{\text{fill}} \quad (12)$$

274 where c_{cut} and c_{fill} are the unit cost of cut and fill per cubic meter, respectively.

275 The right-of-way cost C_{RIG} is related to the right-of-way area occupied by the metro track and
 276 the unit right-of-way cost, which is computed by

$$277 \quad C_{\text{RIG}} = \sum_{s=0}^S \Delta s \times D_w \cdot c_{\text{right}}^s (h_{\text{tra}}^s) \quad (13)$$

278 where c_{right}^s denotes the unit right-of-way cost at horizontal location s , which is a function of with
 279 regard to the metro track elevation.

280 The station cost C_{STA} is determined by the station area and the unit construction cost of the
 281 station. This is represented by Eq. (14) as follows:

$$282 \quad C_{\text{STA}} = \sum_{n=1}^N M_{\text{sta}} \cdot c_{\text{sta}}^n (h_{\text{tra}}^s) \quad (14)$$

283 where M_{sta} denotes the area of metro station, and c_{sta}^n the unit construction cost of the n^{th} metro
 284 station, which is related to the elevation of the metro track in the station area.

285 3.1.3 Constraints

286 The VPIs between any two slopes must satisfy various geometric constraints and geographical
 287 requirements. The geometric specifications on the metro design, which is referred as to ‘‘Code for
 288 Design of Metro (CDM)’’ in China, specifies the requirements of metro alignment design. The
 289 geometric specifications and geographical requirements should be treated as constraints when
 290 minimizing the objective function.

291 (1) Geometric constraints

292 1) The minimum slope length within station area

293 According to the CDM, the slope length within station area must be no less than the platform
 294 length of metro station, as shown in Fig. 4(a). This constraint can be represented by formula (15)

295
$$\begin{cases} X_{k+1} - X_{sta}^n \geq L_p / 2 \\ X_{sta}^n - X_k \geq L_p / 2 \end{cases}, \forall n \in \{1, 2, \dots, N\}, k \in \{1, 2, \dots, K\}, \text{if } X_k < X_{sta}^n < X_{k+1} \quad (15)$$

296 where N is the total number of stations; X_{sta}^n denotes the X coordinate of the central point of the n^{th}
 297 station; L_p denotes the platform length of stations.

298 2) The maximum and minimum slope gradient within station area

299 Considering the requirements of good drainage and safe parking, the gradient of any slope i_k
 300 within a station area must be selected from an integer set Q (see Fig. 4(a)). The constraint is
 301 represented by

302
$$i_k = \frac{Y_{k+1} - Y_k}{X_{k+1} - X_k} \in Q, \forall n \in \{1, 2, \dots, N\}, k \in \{1, 2, \dots, K\}, \text{if } X_k < X_{sta}^n < X_{k+1} \quad (16)$$

303 3) The minimum slope length beyond station area

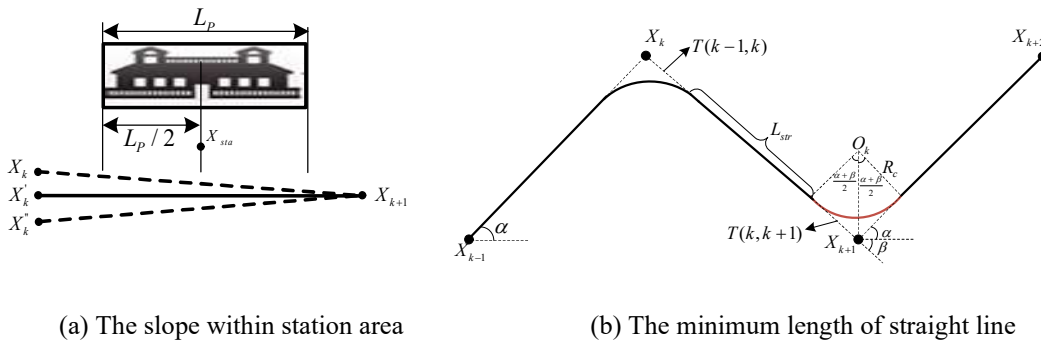
304 The length of any slope outside the station area must be no less than the train length. The train
 305 never runs over more than two slopes at one time for driving safety and passenger comfort. This
 306 constraint is represented by

307
$$L_T \leq X_{k+1} - X_k, \forall n \in \{1, 2, \dots, N\}, k \in \{1, 2, \dots, K\}, \text{if } X_{sta}^n < X_k \text{ and } X_{k+1} < X_{sta}^{n+1} \quad (17)$$

308 4) The maximum and minimum slope gradient beyond station area

309 The gradient of any slope beyond the station area should not exceed i_{\max} , subject to the traction
 310 performance of train motors. Meanwhile, the gradient should also be no less than i_{\min} to facilitate
 311 drainage in tunnels. The constraint is represented by

312
$$i_{\min} \leq \frac{Y_{k+1} - Y_k}{X_{k+1} - X_k} \leq i_{\max}, \forall n \in (1, N), k \in \{1, 2, \dots, K\}, \text{if } X_{sta}^n < X_k \text{ and } X_{k+1} < X_{sta}^{n+1} \quad (18)$$



314 (a) The slope within station area (b) The minimum length of straight line
 315 Fig. 4. Illustration of constraints 1), 2) and 5).

316 5) The minimum length of straight lines between adjacent vertical curves

317 According to the CDM, when the gradient difference between two adjacent slopes reaches 2‰,
 318 a vertical curve must be set at VPI to reduce the vibrations of train movement, as shown in Fig. 4(b).
 319 To further avoid the superposition of train vibrations, the length of the straight line between any two

320 vertical curves should be no less than a minimum value. The constraint can be expressed as
 321
$$X_{k+1} - X_k \geq T(k-1, k) + T(k, k+1) + L_{str}^{\min}, \forall k \in \{1, 2, \dots, K\} \quad (19)$$

322 where L_{str}^{\min} is the minimum length of the straight line; $T(k-1, k)$ denotes the tangent length of the
 323 vertical curve between the $(k-1)^{th}$ and the k^{th} slopes, and $T(k, k+1)$ denotes that between the k^{th} and
 324 the $(k+1)^{th}$ slopes.

325 As illustrated in Fig. 4(b), the relation between the tangent length, the radius of the vertical
 326 curve and the coordinates of VPI can be represented by Eq. (20):

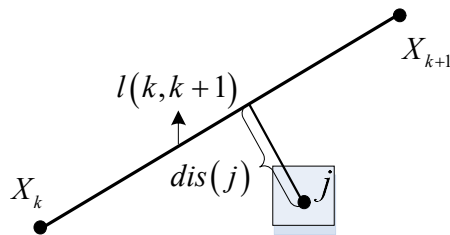
$$\begin{aligned}
 T(k-1, k) &= R_c \times \tan\left[\frac{1}{2} \cdot (\alpha + \beta)\right] \approx \frac{1}{2} \cdot R_c \cdot \tan(\alpha + \beta) \\
 &\approx \frac{1}{2} \cdot R_c \cdot \frac{\tan \alpha + \tan \beta}{1 - \tan \alpha \times \tan \beta} \approx \frac{1}{2} \cdot R_c \times (\tan \alpha + \tan \beta) \\
 &\approx \frac{1}{2} \cdot R_c \cdot [\tan \alpha - \tan(\pi - \beta)] \\
 &= \frac{1}{2} \cdot R_c \cdot \left| \frac{Y_{k+1} - Y_k}{X_{k+1} - X_k} - \frac{Y_k - Y_{k-1}}{X_k - X_{k-1}} \right|
 \end{aligned} \quad (20)$$

328 (2) Geographic restrictions

329 For safety purposes, the metro vertical alignment design must avoid the drift-sand and sludge
 330 layers that are not suitable for tunnel construction and must bypass underground facilities (such as
 331 oil pipelines or gas pipelines).

332 Let J denote the set of the points of the restricted spaces. For any restricted point $j \in J$, the
 333 minimal distance $dis(j)$ between the metro track and the restricted point should be larger than an
 334 acceptable value ε (see Fig. 5). This can be expressed by formula (21). The minimum distance
 335 $dis(j)$ between the metro track and the restricted point can be computed with the Algebraic Method,
 336 which is the formula for finding the shortest distance from a point to a line.

$$337 \quad dis(j) > \varepsilon, \forall j \in J \quad (21)$$



338
 339 Fig. 5. Explanation of the constraints of geographic restrictions.

340 3.2 Energy-efficient train control

341 Given the decisions from the first stage, the second-stage program determines the optimal train

342 speed profile by considering the annual total traction energy cost in both uphill and downhill
 343 directions, which is expressed in Eq. (22). The model is developed based on an optimal train control
 344 strategy composed of maximum acceleration, cruising, coasting, and maximum braking. The train
 345 speed profile is optimized by searching the switching points from the accelerating phase to the
 346 cruising phase a_j^1 and from the cruising phase to the coasting phase a_j^2 (Scheepmaker and Goverde,
 347 2015), in which j denotes the index of interstation track of a metro line.

$$348 \quad E(X_k, Y_k) = \tau \cdot N_T \cdot \sum_{j=1}^{N-1} [\min E_{\text{TRA}}^u(j) + \min E_{\text{TRA}}^d(j)] \quad (22)$$

349 where the ratio τ denotes the unit cost of electricity; N_T represents the average number of one-
 350 direction train trips per year; $E_{\text{TRA}}^u(j)$ denotes the traction energy consumption of one train trip in
 351 the uphill direction of the j^{th} interstation track. $E_{\text{TRA}}^d(j)$ denotes the traction energy consumption of
 352 one train trip in the downhill direction of the j^{th} interstation track.

353 The traction energy consumption in the uphill direction of the j^{th} interstation track $E_{\text{TRA}}^u(j)$ in
 354 Eq. (22) can be computed by multiplying the train traction force over horizontal distance s , which
 355 is expressed as:

$$356 \quad E_{\text{TRA}}^u(j) = \frac{1}{\eta} \cdot \int_0^S F_{\text{tra}}^s ds \quad (23)$$

357 where S is the total length of the j^{th} interstation track; F_{tra}^s denotes the train traction force at location
 358 s , and η the conversion factor from electricity to kinetic energy.

359 The second-stage model is subject to the following constraints. First, to provide a sufficient
 360 operating service and meet the passenger demand, the total running time should not exceed the
 361 maximum allowable running time T .

$$362 \quad \int_0^S \frac{S}{v_s} ds \leq T \quad (24)$$

363 Then, according to Newton's second law, the following three constraints should be obeyed for
 364 train movements.

$$365 \quad \frac{dv(s)}{dt(s)} = \frac{F_{\text{tra}}^s - F_{\text{bra}}^s - w_0(v_s) - w_g(s) - w_c(s)}{M \cdot (1 + \delta)} \quad (25)$$

$$366 \quad w_0(v_s) = (\varphi_0 + \varphi_1 \cdot v_s + \varphi_2 \cdot v_s^2) \cdot M \cdot g \quad (26)$$

$$367 \quad w_g(s) = \left(\sum_{k=1}^K i_k^s \cdot \frac{L_g^{k,s}}{L_T} \right) \cdot M \cdot g \quad (27)$$

$$368 \quad w_c(s) = \left(\frac{600}{R_s} \cdot \frac{L_c^s}{L_T} \right) \cdot M \cdot g \quad (28)$$

369 where F_{bra}^s denotes the train braking force at location s , δ denotes the rotational inertia of the train,

370 M denotes the train mass; v_s represents the train speed at location s ; φ_0 , φ_1 and φ_2 , are coefficients
371 of the Davis Equation (Davis, 1926), which are provided by rolling stock manufacturers; i_k^s and $L_g^{k,s}$
372 are, respectively, the gradient and length of k^{th} slope upon which the train is at location s ; L_T denotes
373 the train length; R_s and L_c^s denote the radius and length of horizontal curve the train covers at location
374 s respectively, which are known from the pre-determined horizontal alignment of metro track.

375 Train traction and braking force at any location are given by Eqs. (29) and (30),:

$$376 \quad F_{\text{tra}}^s = \begin{cases} F_{\text{tra}}^{\max}(v_s), & \text{if } 0 \leq s \leq a_j^1 \\ \max[0, w_0(v_s) + w_g(s) + w_c(s)], & \text{if } a_j^1 < s \leq a_j^2 \\ 0, & \text{if } a_j^2 < s \leq S \end{cases} \quad (29)$$

$$377 \quad F_{\text{bra}}^s = \begin{cases} 0, & \text{if } 0 \leq s \leq a_j^1 \\ \min[0, -w_0(v_s) - w_g(s) - w_c(s)], & \text{if } a_j^1 < s \leq a_j^2 \\ 0, & \text{if } a_j^2 < s \leq a_j^3 \\ F_{\text{bra}}^{\max}(v_s), & \text{if } a_j^3 < s \leq S \end{cases} \quad (30)$$

378 where $F_{\text{tra}}^{\max}(v_s)$ and $F_{\text{bra}}^{\max}(v_s)$ denote the maximum traction and braking forces of a train at a speed of
379 v_s , respectively; a_j^3 is the switching point from the coasting phase to the braking phase.

380 Considering the riding comfort for passengers (especially standing ones), train speed
381 acceleration is limited within a reasonable range.

$$382 \quad \underline{a} \leq \frac{dv(s)}{dt(s)} \leq \bar{a} \quad (31)$$

383 Train speed at the origin and terminal of each inter-station track must be 0 km/h, as represented by
384 Eq. (32):

$$385 \quad \begin{cases} v_0 = 0 \\ v_s = 0 \end{cases} \quad (32)$$

386 Finally, for operational safety, the train speed must not exceed the speed limits at any position,
387 which is expressed as:

$$388 \quad v_s \leq v_s^{\text{limit}} \quad (33)$$

389 where v_s^{limit} denotes the limit speed at location s .

390 The traction energy consumption in the j^{th} interstation track in the downhill direction $E_{\text{TRA}}^d(j)$
391 can also be optimized by using this method. For simplicity, we do not present the detailed
392 formulation.

393 4 Solution approach

394 In this section, we design an iterative approach for solving the two-stage program involving

395 both the optimization of metro vertical alignment and train speed profile. We first introduce the
396 structure of the iterative approach. Then, we propose a DP algorithm with a backward method to
397 optimize the vertical alignment given a train speed profile.

398 **4.1 Iterative approach**

399 The iterative approach combines the BF algorithm and the DP algorithm, whose structure is
400 shown in Fig. 6. The DP algorithm with a backward search method solves the first-stage program
401 on the vertical alignment optimization given a train speed profile. Given a vertical alignment
402 scheme, the BF algorithm solves the second-stage program to find the train speed profile leading to
403 minimal traction energy consumption. The BF algorithm searches for the optimal switching points
404 of the train among the accelerating phase, cruising phase and coasting phase, following the control
405 sequence of maximum acceleration, cruising, coasting, and maximum braking. The specific steps
406 of the BF algorithm are provided in Zhou et al (2018). With the iterative approach, the interaction
407 of the vertical alignment and train speed profile can be considered.

408 As shown in Fig. 6, initially, the train speed profile is optimized by the BF algorithm given a
409 flat track. During the iterations, the vertical alignment is solved by the DP algorithm given the
410 optimized train speed profile. Then, the train speed profile is optimized given the vertical alignment
411 scheme and the optimized profile will be forwarded to the first-stage model for the following vertical
412 alignment optimization. The vertical alignment and train speed profile are iteratively optimized until
413 the difference between the train speed profiles in two consecutive iterations is rather small. Here we
414 set the terminal condition that the speed difference at every location of the train inter-station run is
415 less than 1 km/h.

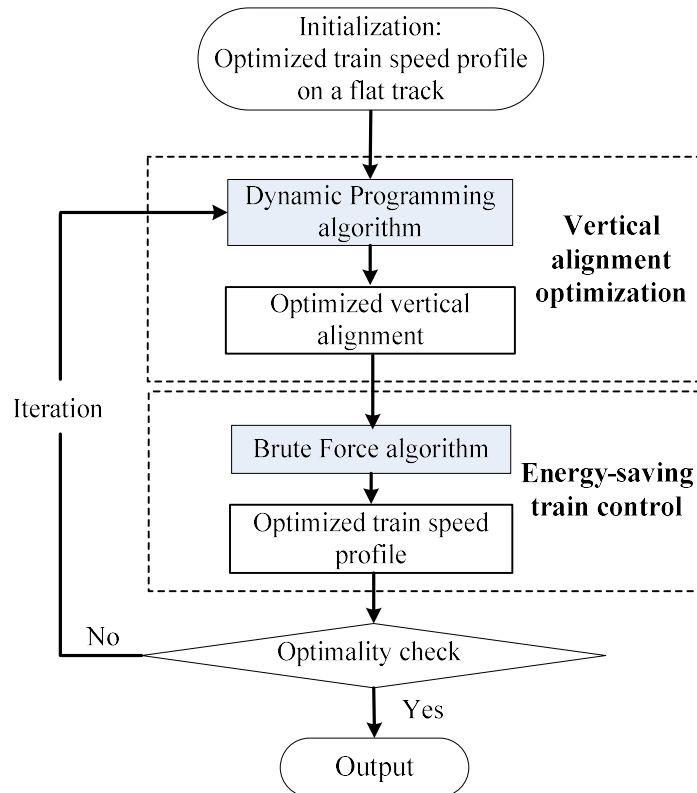


Fig. 6. Procedure of the iterative approach.

4.2 Dynamic programming algorithm

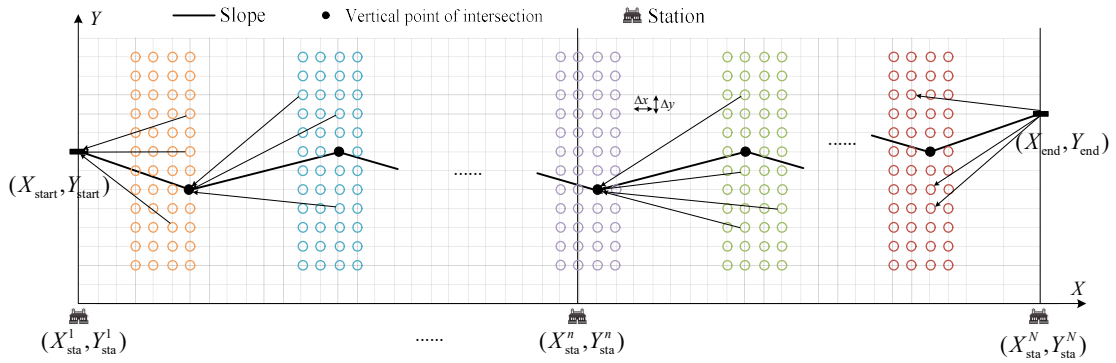
4.2.1 The framework of the DP algorithm

It is very challenging to find the exact solution to the first-stage model on vertical alignment optimization. The complexity of the proposed model stems from two aspects. First, the model has a nonlinear objective function due to the construction costs. For example, the bridge cost is nonlinearly related to the track elevation. The track elevation affects both the length of the bridges and the unit bridge cost per meter, as the unit bridge cost is not a fixed value but varies depending on the bridge height. In other words, the objective function involves a product of two decision variables. Moreover, the track elevation has a nonlinear impact on the number of bridge abutments, which makes the model even harder to solve. On the other hand, the solution space of the proposed model is fairly large for a real-world metro line. The decision variables of the model are the geographical location of VPIs of the metro line. In a continuous search area, the feasible location of a VPI is numerous. For a real-world metro line with hundreds of VPIs, the solution space of the model can be extremely large, which makes it quite difficult to solve.

In this section, we design a DP algorithm with a backward search method to solve the first-stage model on vertical alignment optimization. The DP algorithm has two advantages in solving

434 this model. First, the DP algorithm is a powerful approach to handle nonlinear programming models
 435 (Coaker, 1965), which provides an alternative to solve for an exact solution. Moreover, the proposed
 436 model can be transformed into a multi-stage decision model for determining the coordinates of VPIs,
 437 which fit the DP algorithm well. The best solution of the model can be efficiently obtained by
 438 solving and recording the solutions of each sub-model.

439 To build the DP framework, a two-dimensional grid is first developed to discretize the search
 440 space. In the two-dimensional grid, the width and height of a cell are determined beforehand. The
 441 VPIs are restricted to be located at the vertexes of the cells, as shown in Fig. 7. The set of all vertexes
 442 of the cells is denoted by \mathfrak{R} .



443
444 Fig. 7. A two-dimensional grid for the vertical alignment optimization

445 We then transform the vertical alignment optimization problem into a multi-stage decision
 446 problem based on the decisions of the VPI locations. The framework of the DP algorithm could thus
 447 be reformulated in terms of stage, state, decision and cost function.

448 **Stage:** The vertical alignment can be divided into $K+1$ parts by the K VPIs. The vertical
 449 alignment optimization problem can thus be transformed into a multi-stage decision problem with
 450 $K+1$ stages. In the DP algorithm, let k denote the index of the stage.

451 **State:** The state in the DP algorithm is the location of the VPIs. At stage k , the state variable
 452 is represented by the geographic coordinates $(X_k, Y_k) \in \mathfrak{R}$ of the k^{th} VPIs.

453 **Decision:** The decision in the DP algorithm is the action of selecting the next VPI (X_{k+1}, Y_{k+1})
 454 based on the location of the current VPI (X_k, Y_k) . Let $A_{(X_k, Y_k)}$ denote the action space of the state
 455 variable (X_k, Y_k) . Each action $a_k = (X_k, Y_k) \rightarrow (X_{k+1}, Y_{k+1}) \in A_{(X_k, Y_k)}$ will connect the point (X_k, Y_k)
 456 to a point (X_{k+1}, Y_{k+1}) by a slope, and the action must satisfy all the constraints in Section 3.3. The
 457 final metro vertical alignment will be determined by the best set of actions $\mathfrak{A} = \{a_0^*, \dots, a_k^*, \dots, a_K^*\}$.

458 **Cost function:** The metro vertical alignment optimization problem can be transformed into the
 459 following a multi-stage decision problem:

460
$$\min C_{\text{TOL}} = \min_{\mathfrak{A}} \sum_{k=0}^K J_k \quad (34)$$

461 where J_k indicates the costs associated with the action a_k , which includes the construction costs
 462 and the train traction energy consumption.

463 According to the Bellman principle of optimality (Bellman, 1966), the recurrence equation of
 464 a backward dynamic program is expressed as:

465
$$C_{\text{TOL}}^*(X_{k-1}, Y_{k-1}) = \min_{a_k^*} [J_k + C_{\text{TOL}}^*(X_k, Y_k)] \quad (35)$$

466 where $C_{\text{TOL}}^*(X_{k-1}, Y_{k-1})$ denotes the minimum cumulative costs from the state (X_{k-1}, Y_{k-1}) to the state
 467 $(X_{\text{end}}, Y_{\text{end}})$, and $C_{\text{TOL}}^*(X_k, Y_k)$ denotes that from (X_k, Y_k) to $(X_{\text{end}}, Y_{\text{end}})$.

468 4.2.2 Backward search method

469 To solve the best action set of the first-stage model on vertical alignment optimization, a
 470 backward search method is proposed to compute the minimum cumulative costs from the state
 471 $(X_{\text{start}}, Y_{\text{start}})$ to the state $(X_{\text{end}}, Y_{\text{end}})$. As shown in Fig. 7, the backward search method starts at
 472 $(X_{\text{end}}, Y_{\text{end}})$ and ends at $(X_{\text{start}}, Y_{\text{start}})$.

473 Let \square_k denote the set of all current states at stage k . The search process is depicted in Fig. 8.
 474 Let $Pred(X_k, Y_k)$ denote the predecessor state of the state (X_k, Y_k) that causes the minimum
 475 cumulative costs to the state $(X_{\text{end}}, Y_{\text{end}})$.

476 **Step 0.** Initialization: Set stage $k=0$, and $Pred(X, Y) = \emptyset, \forall (X, Y) \in \mathfrak{R}$. Set $C_{\text{TOL}}^*(X_{\text{end}}, Y_{\text{end}}) = 0$
 477 and $C_{\text{TOL}}^*(X, Y) = \infty$ for all states (X, Y) in \mathfrak{R} except $(X_{\text{end}}, Y_{\text{end}})$. Add the state $(X_{\text{end}}, Y_{\text{end}})$ to the set
 478 of current states \square_k .

479 **Step 1.** For each current state $(X, Y) \in \square_k$, compute the corresponding action space $A_{(X, Y)}$.

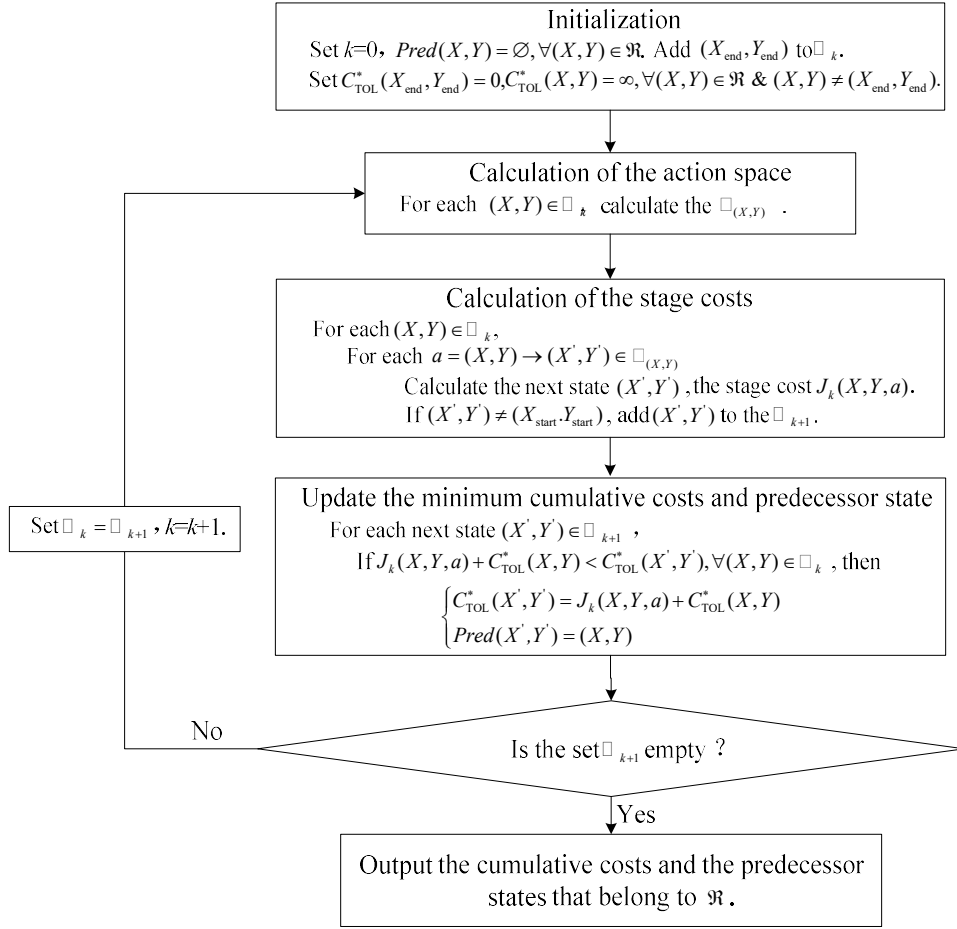
480 **Step 2.** For each current state $(X, Y) \in \square_k$ and for each $a = (X, Y) \rightarrow (X', Y') \in A_{(X, Y)}$, compute
 481 the next state (X', Y') and the stage cost $J_k(X, Y, a)$ between the current and the next state. If the
 482 next state is not the same as the state $(X_{\text{start}}, Y_{\text{start}})$, add the next state to the set \square_{k+1} .

483 **Step 3.** Update the minimum cumulative costs and predecessor state:

484 For each next state $(X', Y') \in \square_{k+1}$, if $J_k(X, Y, a) + C_{\text{TOL}}^*(X, Y) < C_{\text{TOL}}^*(X', Y'), \forall (X, Y) \in \square_k$, then
 485 update the minimum cumulative costs and predecessor state using Eq. (36).

486
$$\begin{cases} C_{\text{TOL}}^*(X', Y') = J_k(X, Y, a) + C_{\text{TOL}}^*(X, Y) \\ Pred(X', Y') = (X, Y) \end{cases} \quad (36)$$

487 **Step 4.** If $\square_{k+1} = \emptyset$, set $\square_k = \square_{k+1}$ and $k=k+1$, then go to Step 1; otherwise output the
 488 cumulative costs and output the predecessor states that belong to \mathfrak{R} .



489

490

Fig. 8. Flowchart of backward dynamic programming search.

491

From the backward search process recorded by the predecessor states, all the states can be
 492 obtained from (X_{start}, Y_{start}) to (X_{end}, Y_{end}) , with the minimum cumulative costs. The best vertical
 493 alignment in the two-dimensional grid can thus be found.

494

5 Case studies

495

The case studies are based on the Guangzhou Metro Line 14 in China. There are seven stations
 496 along the line, which runs from the southwest across the city center to the northeast. Its length is
 497 27.15 km. The trains running on Line 14 consist of four motorized vehicles and two trailers, in
 498 which each motorized vehicle is equipped with four motors. The parameters of the trains are listed
 499 in Table 2. The traction and braking characteristics of a motor of the metro train are shown in Fig.
 500 9.

501

The parameters associated with the constraints are presented in Table 3. Table 4 lists the
 502 parameters of the unit costs in the objective function. The case studies are conducted on a desktop

503 PC with an Intel Core i5-9500F CPU (2.5 GHz), 16GB of RAM, and a Microsoft Windows 10 Pro
 504 64-Bit operating system.

505 Table 2 Parameters of Train A

| Parameter | Value |
|--|------------------------------|
| Train mass (M) | 293.4 t |
| Train length (L_T) | 120 m |
| Number of motors (n_m) | 16 |
| Coefficients of the Davis Equation ($\varphi_0 / \varphi_1 / \varphi_2$) | 1.8214 / 0.030612 / 0.000251 |
| Conversion factor from electricity to kinetic energy (η) | 0.9 |
| Rotational inertia (δ) | 0.38 |

506 Table 3 Parameters of model constraints

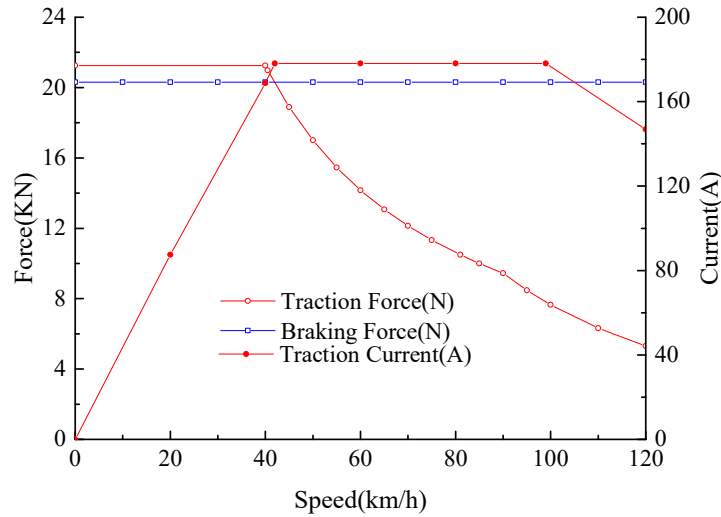
| Description | Value |
|--|---------------------|
| The integer set of the gradient of slope within station area (Q) | {-2‰, 0‰, 2‰} |
| The platform length of metro station (L_p) | 150 m |
| Minimum gradient of slope beyond station area (i_{\min}) | 3‰ |
| Maximum gradient of slope beyond station area (i_{\max}) | 30‰ |
| The radius of the vertical curve (R_c) | 5000 m |
| Minimum length of straight line between adjacent vertical curves (L_{str}^{\min}) | 20 m |
| Minimum difference between track and restricted space (ε) | 1 m |
| The average number of one-direction train trips per year (N_T) | 67525 |
| The maximum bridge length (s_{maxb}) | 20 m |
| Station area (M_{sta}) | 3000 m ² |
| Number of compounding years of metro economic life (n) | 60 years |
| Interest rate per year (i) | 5 % |
| The width of metro track alignment (D_w) | 20 m |
| The minimum bridge height (h_{minb}) | 10 m |
| The minimum depth of tunnel (h_{mint}) | 13 m |

507 Table 4 Unit costs

| Items | Value | Items | Value |
|--|--------------------------|---|-------------|
| Electricity (τ) | 1.0 CNY/kWh | Metro track (c_{tra}) | 20000 CNY/m |
| Tunnel (c_{tun}) | 80000 CNY/m | One tunnel portal (c_{por}) | 500000 CNY |
| Cutting earthwork (c_{cut}) | 35 CNY/m ³ | One abutment of bridge (c_{abu}) | 40000 CNY |
| Filling earthwork (c_{fill}) | 40 CNY/m ³ | ($H_{\text{bri}} \leq 10\text{m}$) Bridge (c_{bri}) | 42000 CNY/m |
| Underground station (c_{sta}) | 40000 CNY/m ² | ($10\text{m} < H_{\text{bri}} \leq 15\text{m}$) Bridge (c_{bri}) | 54600 CNY/m |
| Elevated station (c_{sta}) | 20000 CNY/m ² | ($15\text{m} < H_{\text{bri}} \leq 20\text{m}$) Bridge (c_{bri}) | 67200 CNY/m |

| | | | |
|---|--------------------------|--|--------------------------|
| Ground station (c_{sta}) | 10000 CNY/m ² | ($H_{bri} > 20$ m) Bridge (c_{bri}) | 79800 CNY/m |
| ($s \leq 14$ km) Right-of-way cost of the underground line (c_{right}) | 2000 CNY/m ² | ($s > 14$ km) Right-of-way cost of the underground line (c_{right}) | 10000 CNY/m ² |
| ($s \leq 14$ km) Right-of-way cost of the ground line (c_{right}) | 30000 CNY/m ² | ($s > 14$ km) Right-of-way cost of the ground line (c_{right}) | 20000 CNY/m ² |
| ($s \leq 14$ km) Right-of-way cost of the elevated line (c_{right}) | 13000 CNY/m ² | ($s > 14$ km) Right-of-way cost of the elevated line (c_{right}) | 3000 CNY/m ² |

508



509

Fig. 9. Traction and braking performance of a train motor.

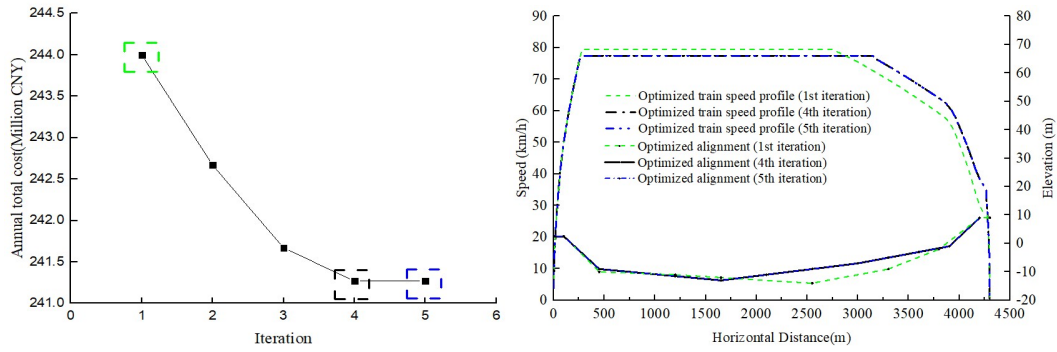
510

5.1 Performance of the solution approach

5.1.1 The convergence of the iterative approach

513 In this subsection, we test the convergence of the proposed iterative approach in optimizing
514 the vertical alignment of Guangzhou Metro Line 14. The convergence process of the iterative
515 approach is illustrated in Fig. 10(a). The iterative approach achieves convergence after 5 iterations.
516 By the first optimization, the annual total cost is reduced to 244.00 million. With the iterations, the
517 annual total cost is further decreased to 241.27 million CNY.

518 Taking the first inter-station track as an example, we give the optimized train speed profile and
519 the vertical alignment in the first and last two iterations (see Fig. 10(b)). It can be seen that the
520 optimized train speed profiles at the last two iterations are overlapped, which indicates the
521 convergence of the iterative approach in solving the two-stage program.



522

523 (a) Costs changes in successive iterations

(b) The optimized speed profile and vertical alignment

524

Fig. 10. The convergence of the iterative approach.

525

5.1.2 The efficiency of the DP algorithm

526

527

528

529

530

531

532

533

534

535

536

537

538

539

540

We further analyze the efficiency of the DP algorithm in solving the first-stage model on vertical alignment optimization, for a given train speed profile with a maximum cruising speed of 78 km/h. The performance of the DP algorithm depends on the cell size in the grid. Smaller cell size in the grid can improve computation accuracy and thus solutions, but also increases the number of decision variables and computation time. Therefore, different cell sizes are set, in which the width of cells Δx varies from 150 m to 50 m, and the height of cells Δy varies from 1.5 m to 0.5 m.

The computation results are presented in Table 5. With the decrease of the cell width and height, the search space is enlarged, and thus the computation time is increased greatly from 0.1 hours to 14 hours. The annual total costs are also decreased from 259.09 million to 252.78 million CNY. When the width and height of the cell are set as $\Delta x=50$ m and $\Delta y=0.5$ m, the annual total costs are 252.78 million CNY, but the computation time is too long at 14 hours. When the cell size is increased to $\Delta x=100$ m and $\Delta y=1$ m, the annual total costs are increased to 255.19 million CNY by only 0.94%, which is also a satisfactory solution, but the computation time can be significantly shortened to 2 hours. In a nutshell, the quality of the solutions obtained by the DP algorithm can be enhanced if the accuracy of the two-dimensional grid is improved.

541

Table 5 The performance of the DP algorithm under different cell sizes in the grid

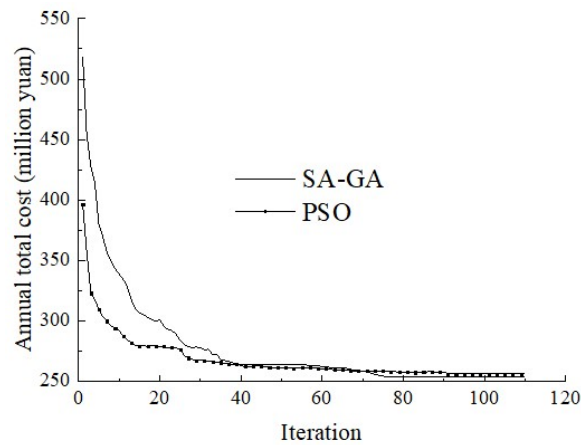
| Cell width Δx (m) | Cell height Δy (m) | Annual total costs (million CNY) | Computation Time (h) |
|---------------------------|----------------------------|----------------------------------|----------------------|
| 50 | 0.5 | 252.78 | 14.0 |
| 50 | 1.0 | 252.81 | 10.0 |
| 50 | 1.5 | 254.00 | 6.0 |
| 100 | 0.5 | 254.86 | 4.0 |
| 100 | 1.0 | 255.19 | 2.0 |
| 100 | 1.5 | 255.70 | 1.5 |

| | | | |
|-----|-----|--------|-----|
| 150 | 0.5 | 257.62 | 0.5 |
| 150 | 1.0 | 258.16 | 0.2 |
| 150 | 1.5 | 259.09 | 0.1 |

542

543 For comparison, two heuristic algorithms in the existing studies are applied, which include the
544 SA-GA (Sun et al., 2020) and the PSO algorithm (Shafahi and Bagherian, 2013). Unlike the DP
545 algorithm using the two-dimensional grid, the two heuristic algorithms optimize the geographical
546 locations of the VPIs in a continuous search space. The parameters are set as follows. In the SA-
547 GA, the population size, the crossover rate, and the mutation rate are set as 250, 0.8, and 0.15,
548 respectively. In the PSO, the population size, the decreasing inertia weight, the maximum velocity,
549 and the two accelerator coefficients are set as 250, 0.6, 0.3, 2 and 2, respectively. The two heuristic
550 algorithms are tested using the same computation time as the DP algorithm.

551 The convergence process of the SA-GA and PSO is illustrated in Fig. 11. With the computation
552 time increases, the solution quality of the SA-GA and the PSO is increased, and the annual total
553 costs is decreased from 382.63 million to 253.22 million CNY, and from 324.79 million to 255.43
554 million CNY, respectively. The SA-GA can reach a better solution than the PSO after about 50
555 iterations. Fig. 12 illustrates the vertical alignments optimized by the DP, SA-GA and PSO.
556 Compared to the vertical alignment optimized by the PSO, the alignment optimized by the SA-GA
557 is closer to that optimized by the DP algorithm.



558

559 Fig. 11. Annual total costs changes in successive iterations of the SA-GA and the PSO.

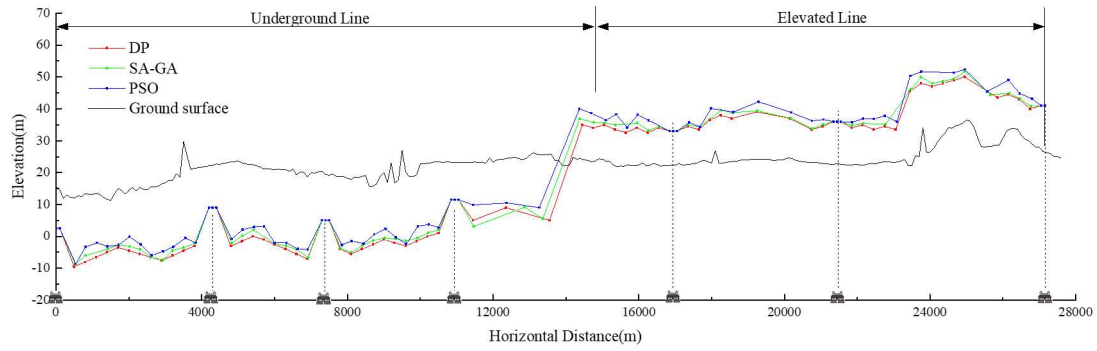


Fig. 12. The vertical alignments optimized by the DP, SA-GA and PSO.

As shown in Table 6, the DP algorithm outperforms the two heuristic algorithms, i.e., SA-GA and PSO, in the case study. Given the same computation time, the annual total costs associated with the vertical alignment produced by the DP algorithm are less than that by the heuristic algorithms. Within two hours, the DP algorithm can produce much better solutions as the heuristic algorithms cannot search for high-quality solutions in such a short period of time. After more than 10 hours of computation, the DP algorithm also showed better performance as it should find the optimal solution in a high-accuracy two-dimensional grid. When the computation time is 4 or 6 hours, the annual total costs computed by the DP algorithm is slightly greater than that by the SA-GA; the gap between the two algorithms is 0.34% and 0.17%, respectively, due to the accuracy loss when splitting the grid during the implementation of the DP algorithm.

Table 6 Comparison between the DP algorithm and heuristic algorithms

| Computati on Time (h) | Annual total cost (Million CNY) | | Saving rate | Annual total cost (Million CNY) | | Saving rate |
|-----------------------------|------------------------------------|--------|----------------|------------------------------------|--------|----------------|
| | DP | SA-GA | | DP | PSO | |
| 14.0 | 252.78 | 253.22 | 0.17% | 252.78 | 255.43 | 1.04% |
| 10.0 | 252.81 | 253.22 | 0.16% | 252.81 | 256.38 | 1.39% |
| 6.0 | 254.00 | 253.58 | -0.17% | 254.00 | 259.55 | 2.14% |
| 4.0 | 254.86 | 253.99 | -0.34% | 254.86 | 262.26 | 2.82% |
| 2.0 | 255.19 | 262.49 | 2.78% | 255.19 | 266.99 | 4.42% |
| 1.5 | 255.70 | 268.38 | 4.72% | 255.70 | 269.74 | 5.21% |
| 0.5 | 257.62 | 307.97 | 16.35% | 257.62 | 280.2 | 8.06% |
| 0.2 | 258.16 | 361.39 | 28.56% | 258.16 | 297.6 | 13.25% |
| 0.1 | 259.09 | 382.63 | 32.29% | 259.09 | 324.79 | 20.23% |

5.2 The optimized vertical alignment

In this subsection, we compare the experienced designers' manual vertical alignment and the

577 optimized vertical alignments with different optimization objectives to illustrate the effectiveness
 578 of the two-stage optimization program. The maximum allowable train running time is set as 1474s
 579 for 6 inter-station tracks. The width and height of the cell in the DP algorithm are set as $\Delta x=50$ m
 580 and $\Delta y=0.5$ m. Hereafter, we refer to the optimized alignment with the minimal construction costs
 581 as “construction cost-oriented alignment”, the optimized alignment with the minimal traction energy
 582 consumption as “traction energy-oriented alignment”, and the optimized alignment with minimizing
 583 both the traction energy consumption and construction costs by the two-stage program as “total
 584 cost-oriented alignment”.

585 With the different vertical alignments, the results of the annual construction costs (ACC), the
 586 annual traction energy cost (ATEC) and the annual total costs (ATC) is shown in Table 7. Table 8
 587 shows details of the construction costs with the different vertical alignments.

588 Table 7 Costs comparison among different vertical alignments (Million CNY)

| | ACC | ATEC | ATC |
|--------------------------------------|----------------|--------------|----------------|
| Manual alignment | 226.32 | 30.42 | 256.74 |
| Construction cost-oriented alignment | 214.10(-5.4%) | 31.27(+2.8%) | 245.37(-4.4%) |
| Traction energy-oriented alignment | 433.56(+91.6%) | 27.55(-9.4%) | 461.11(+79.6%) |
| Total cost-oriented alignment | 213.15(-5.8%) | 28.12(-7.6%) | 241.27(-6.0%) |

589 Table 8 Construction costs comparison among different vertical alignments (Million CNY)

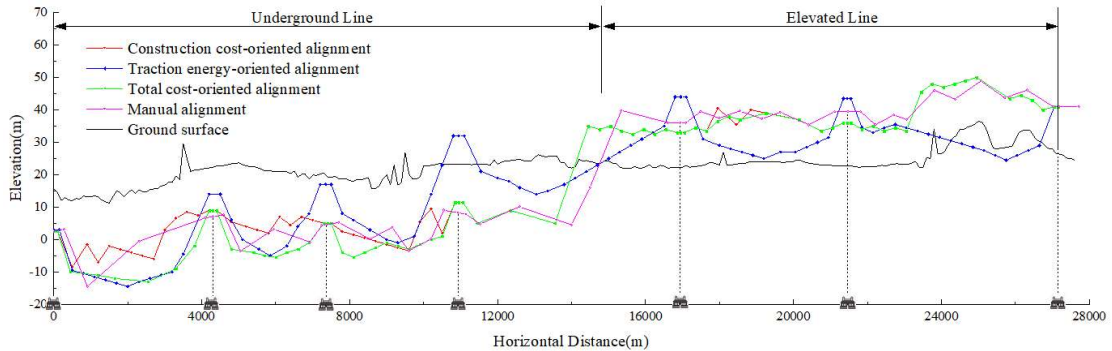
| | C_{TRA} | C_{BRI} | C_{TUN} | C_{EAR} | C_{RIG} | C_{STA} | ACC |
|--------------------------------------|-----------|-----------|-----------|-----------|-----------|-----------|--------|
| Manual Alignment | 20.02 | 49.65 | 40.17 | 8.14 | 89.98 | 18.36 | 226.32 |
| Construction cost-oriented alignment | 20.02 | 44.88 | 35.74 | 6.70 | 92.62 | 14.13 | 214.10 |
| Traction energy-oriented alignment | 20.02 | 10.10 | 19.23 | 59.23 | 312.77 | 12.21 | 433.56 |
| Total cost-oriented alignment | 20.02 | 46.15 | 34.51 | 6.70 | 92.04 | 13.73 | 213.15 |

590

591 According to Table 7, compared with the manual alignment, the construction cost-oriented
 592 alignment decreases the construction costs by 5.4% and the traction energy-oriented alignment
 593 decreases the traction energy cost by 9.4%. The two alignments provide the minimal cost of
 594 construction and traction energy consumption, respectively. However, the construction cost-
 595 oriented alignment increases the traction energy cost by 2.8%, and the traction energy-oriented
 596 alignment significantly increases the construction costs by 91.6%. Based on that, the annual total
 597 costs are reduced by 4.4% in the construction cost-oriented alignment, whereas they are increased
 598 by 79.6% in the traction energy-oriented alignment. This shows that the optimization of the vertical
 599 alignment cannot neglect the construction cost.

600 Besides, the total cost-oriented alignment reduces both the construction costs and the traction
 601 energy cost by 5.8% and 7.6%, respectively. The total costs can thus be reduced by 6.0%, which is
 602 larger than the decrease rate of 4.4% in the construction cost-oriented alignment. Compared with
 603 the construction cost-oriented alignment, the total cost-oriented alignment can reduce the traction
 604 energy cost yet with a very slight increase of the construction cost. This result illustrates the good
 605 performance of the two-stage program in reducing construction costs and traction energy.

606



607

608 Fig. 13. The manual and optimized vertical alignments with different optimization objectives.

609

610 The manual and optimized alignments are shown in Fig. 13. It can be seen that, except for the
 611 traction energy-oriented alignment, the other alignments are built underground when the horizontal
 612 distance is less than 14000 m and turn to be elevated when their distance is longer than 14000 m.
 613 The reason is that the right-of-way cost is fully considered in the construction cost-oriented
 614 alignment and the total cost-oriented alignment. The metro vertical alignment should be built
 615 underground as the unit right-of-way cost of an elevated or ground metro line is high when the
 616 horizontal distance is between 0 and 14000 m (as shown in Table 4). Similarly, when the horizontal
 617 distance is between 14000 and 27150 m, the unit right-of-way cost of an elevated line is lower than
 618 an underground or ground line, and a bridge is preferable when the horizontal distance exceeds
 619 14000 m.

620

621 A steep downhill slope in the train running direction contributes to reducing the required
 622 traction energy during the train's acceleration process. For the underground line, as the unit
 623 construction costs of the tunnel is unrelated to the depth of the tunnel (Patino-Ramirez et al., 2020),
 624 it is proper to set steep slopes near the station area for traction energy saving. As shown in Fig. 13,
 625 the gradient near the station area of the traction energy-oriented alignment is steep. However, the
 626 steep downhill slope increases construction costs when the metro line is built on the bridge. As
 shown in Fig. 13, to reduce construction cost, the gradient near the station area of the total cost-

627 oriented alignment is flat when it is built on the bridge.

628 Based on the analyses, two broad conclusions on metro vertical alignment design can be
629 summarized as follows: 1) for an underground metro line, steep downhill slopes near a station in
630 the train running direction can assist trains in accelerating and reducing the traction energy
631 consumption; 2) for an elevated metro line, a flat vertical alignment rather than steep slopes reduces
632 life-cycle cost, as the construction costs reduction exceeds the increment in traction energy cost.

633 **5.3 Sensitivity analysis on the maximum allowable running time**

634 Given the vertical alignment, the maximum allowable train running time has a significant
635 influence on the train traction energy. In this section, we analyze the impact of the maximum
636 allowable train running time on the energy performance of the optimized vertical alignment. Firstly,
637 we optimize the vertical alignment by the two-stage optimization program based on a preset
638 maximum train running time (i.e., 1474s). Then, given the optimized vertical alignment, we further
639 optimize train speed profile by the second-stage model under different maximum allowable running
640 times.

641 Table 10 gives the ATEC of the manual and optimized alignment for various train speed
642 profiles limited by different train running times. With the preset train running time, the optimized
643 vertical alignment decreases the ATEC by 9.43%, compared to the manually designed vertical
644 alignment. When the train running time decreases by 8% and increases by 8% and 16% from the
645 preset one, the energy-saving rates of the optimized vertical alignments are 4.61%, 6.38%, and
646 6.41%, respectively. We can see that the energy performance of the optimized vertical alignment is
647 better than that of the manually designed vertical alignment for different train running times.

648

649 Table 10 Annual traction energy cost comparison under different running times

| Maximum allowable running time (s) | ATEC (Million CNY) | | Energy-saving rate (%) |
|---------------------------------------|--------------------|--------------|---------------------------|
| | Manual | Optimized | |
| 1474 | 30.42 | 27.55 | 9.43 |
| 1354 (-8%) | 41.44 | 39.53 | 4.61 |
| 1594 (+8%) | 27.59 | 25.83 | 6.38 |
| 1714 (+16%) | 25.42 | 23.79 | 6.41 |

650

651 **6 Conclusions**

652 Metro vertical alignment design is a complex engineering problem since it has many nonlinear
653 constraints and a very large solution space. Existing studies on this subject mostly employed
654 heuristic algorithms to obtain a near-optimal solution, and the stability of the solution would not be
655 guaranteed. This paper proposes an iterative approach for solving the vertical alignment
656 optimization problem, considering both the construction costs and traction energy consumption. The
657 following are the main contributions of this paper:

- 658 1. An integrated two-stage optimization program is proposed involving both metro vertical
659 alignment and train speed profile, which considers a wide variety of constraints in terms of both
660 geographical and geometrical requirements around the metro line area. It ensures the practical
661 applicability of the resulting vertical alignment to minimize the costs of construction and
662 traction energy.
- 663 2. An iterative approach is proposed to solve the two-stage program. A dynamic programming
664 (DP) algorithm is designed based on a two-dimensional grid system, where the vertical
665 alignment optimization problem is transformed into a multi-stage decision problem, given the
666 vertical point of intersection (VPI) locations. In that way, a backward search method is proposed
667 to search for the best vertical alignment given an energy-efficient train speed profile.
- 668 3. The DP algorithm was tested with real data from Guangzhou Metro Line 14, and the results
669 were compared with those of two heuristic algorithms. The results demonstrated that the DP
670 algorithm generally provides better solution quality within the same computation time. The
671 optimized vertical alignment based on our proposed model and the iterative approach could
672 help achieve a 6.0% reduction in the total costs of construction and traction energy.
- 673 4. From our study, we can reach a few broad conclusions about metro vertical alignment, which
674 may serve as a useful reference for its practical design: 1) for an underground metro line, steep
675 downhill slopes near a station in the train running direction can assist trains in accelerating and
676 reducing the traction energy consumption; 2) for an elevated metro line, a flat vertical alignment
677 rather than steep slopes leads to a lower life-cycle cost, as the saving on construction costs
678 exceeds the increment on traction energy cost.

679 The work presented in this paper focused only on the vertical alignment of metro tracks;
680 however, the metro vertical alignment interacts with its horizontal alignment, which would also
681 affect the construction costs and traction energy consumption. Therefore, joint optimization of the
682 horizontal and vertical alignment for the metro tracks is well worth future research efforts.

683

684 **Declaration of Competing Interest**

685 The authors declare that they have no known competing financial interests or personal
686 relationships that could have appeared to influence the work reported in this paper.

687

688 **Acknowledgements**

689 This work was supported by the Fundamental Research Funds for the Central Universities
690 [grant number 2020JBM035] and the National Natural Science Foundation of China [grant number
691 71971016, 72101019]. Qian Wang was supported by the China Scholarship Council
692 (202107090057). The author thanks Guangzhou Metro Design & Research Institute Co., Ltd for the
693 data provided on metro alignment design and construction.

694

695 **References**

- 696 Bababeik, M., Monajjem, M.S., 2012. Optimizing longitudinal alignment in railway with regard to
697 construction and operating Costs. *J. Transp. Eng. ASCE*. 138(11), 1388–1395.
- 698 Bellman, R., 1966. Dynamic programming. *Science*. 153(3731), 34–37.
- 699 Coaker, P.B., 1965. Nonlinear and dynamic programming. *J. Oper. Res. Soc.* 16(3), 392–393.
- 700 Code for Design of Metro. GB 50157–2013, 2013.
- 701 Costa, A.L., Sousa, R.L., Einstein, H.H., 2017. Probabilistic 3D alignment optimization of
702 underground transport infrastructure integrating GIS-based subsurface characterization. *Tunn.*
703 *Undergr. Space. Technol.* 72, 233–241.
- 704 Davis, W J., 1926. The tractive resistance of electric locomotives and cars. *Gen. Electr. Rev.* 29,
705 685–707.
- 706 Duarte, M.A., Sotomayor, P.X., 1999. Minimum energy trajectories for subway systems. *Optim.*
707 *Control Appl. Meth.* 20, 283–296.
- 708 Easa, S.M., 1988. Selection of roadway grades that minimize earthwork cost using linear
709 programming. *Transp. Res. Part A: Pol. Pract.* 22(2), 121–136.
- 710 Fwa, T.F., Chan, W.T., Sim, Y.P., 2002. Optimal vertical alignment analysis for highway design. *J.*
711 *Transp. Eng. ASCE*. 128 (5), 395–402.
- 712 Ghoreishi, B., Shafahi, Y., Hashemian, S.E., 2019. A model for optimizing railway alignment
713 considering bridge costs, tunnel costs, and transition curves. *Urban Rail Transit*. 5(4), 207–224.
- 714 Goktepe, A.B., Lav, A.H., Altun, S.W. 2005. Dynamic optimization algorithm for vertical
715 alignment of highways. *Math. Comput. Appl.* 10(3), 341–350.

716 Goktepe, A.B., Lav, A.H., Altun, S.W., 2009. Method for optimal vertical alignment of highways.
717 Transport. 162 (4), 177–188.

718 Guangzhou Statistics Bureau, 2020. Guangzhou statistical yearbook, China Statistics Press, Beijing.

719 Hare, W., Lucet, Y., Rahman, F., 2015. A mixed-integer linear programming model to optimize the
720 vertical alignment considering blocks and side-slopes in road construction. European. J. Oper.
721 Res. 241(2015), 631–641.

722 Hoang, H., Polis, M., Haurie, A., 1975. Reducing energy consumption through trajectory
723 optimization for a subway network. IEEE. T. Automat. Contr. 20(5), 590–595.

724 Howlett, P., 1990. An optimal strategy for the control of a train. J. Aust. Math. Soc. Series B. 31(4),
725 454–471. doi:10.1017/S0334270000006780.

726 Howlett, P., Pudney, P., Vu, X., 2009. Local energy minimization in optimal train control.
727 Automatica. 45(11), 2692–2698.

728 Jha, M.K., Schonfeld, P., Samanta S., 2007. Optimizing rail transit routes with genetic algorithms
729 and geographic information system. J. Urban. Plan. Dev. 133(3), 161–171.

730 Kim, D.N., Schonfeld, P., 1997. Benefits of dipped vertical alignments for rail transit routes. J.
731 Transp. Eng. ASCE, 123(1), 20–27.

732 Kim, M., Schonfeld, P., Kim, E., 2013. Comparison of vertical alignments for rail transit. J. Transp.
733 Eng. ASCE, 139(2), 230–238.

734 Kim, M., Markovic, N., Kim, E., 2019. A vertical railroad alignment design with construction and
735 operating costs. J. Transp. Eng. ASCE. 145(10), 04019043.

736 Lafortune, S., Polis, M.P., 1983. Interactive computer aided analysis and design of energy efficient
737 subway tunnel trajectories. IFAC Proceedings Volumes. 16, 437–446.

738 Lai, X., Schonfeld, P., 2012. Optimization of rail transit alignments considering vehicle dynamics.
739 Transp. Res. Rec. 2275, 77–87.

740 Li, DW., Dong, XL., Cao, JM., Zhang, SL., Yang, L., 2022. Energy-efficient rail transit vertical
741 alignment optimization: a gaussian pseudo-spectral method. J. Transp. Eng. Part A: Systems.
742 148(1), 04021100.

743 Li, W., Pu, H., Schonfeld, P., Zhang, H., Zheng, X., 2016. Methodology for optimizing constrained
744 3-dimensional railway alignments in mountainous terrain. Transport. Res. Part C: Emerg.
745 Technol. 68(2016), 549–565.

746 Li, W., Pu, H., Zhao, H., Liu, W., 2013. Approach for optimizing 3D highway alignments based on
747 two-stage dynamic programming. J. Softw -Evol. Proc. 8(11), 2967–2973.

748 Patino-Ramirez, F., Layhee, C., Arson, C., 2020. Horizontal directional drilling (HDD) alignment
749 optimization using ant colony optimization. *Tunn. Undergr. Space. Technol.* 103, 103450.

750 Pu, H., Song, T.R., Schonfeld, P., Li, W., Zhang, H., Wang, J., and Peng, X., 2019. A three-
751 dimensional distance transform for optimizing constrained mountain railway alignments.
752 *Comput.-Aided Civ. Infrastruct. Eng.* 34(11), 972–990.

753 Samanta, S., Jha, M.K., 2011. Modeling a rail transit alignment considering different objectives.
754 *Transport. Res. Part A: Pol. Prac.* 45, 31–45.

755 Scheepmaker, G. M. and Goverde, R. M. P. 2015. The interplay between energy-efficient train
756 control and scheduled running time supplements. *J. Rail Transport Plann. Manag.* 5(4), 225–239.
757 doi: 10.1016/j.jrtpm.2015.10.003.

758 Shafahi, Y., Bagherian, M., 2013. A customized particle swarm method to solve highway alignment
759 optimization problem. *Comput.-Aided Civ. Infrastr. Eng.* 28(1), 52–67.

760 Shafahi, Y., Shahbazi, J., 2012. Optimum railway alignment.
761 http://www.uic.org/cdrom/2001/wcrr2001/pdf/sp/2_1_1/2_1_10.pdf.

762 Song, T.R., Pu, H., Schonfeld, P., Li, W., Zhang, H., Ren, Y.H., et al., 2020. Parallel three-
763 dimensional distance transform for railway alignment optimization using OpenMP. *J. Transp.*
764 *Eng. Part A: Systems.* 146(5), 04020029.

765 Song, T. R., Pu, H., Schonfeld, P., Hu, J., Liu, J., 2022. Robust optimization method for mountain
766 railway alignments considering preference uncertainty for costs and seismic risks. *ASCE-ASME*
767 *J. Risk Uncertainty Eng. Syst., Part A: Civ. Eng.* 8(1): 04021077.

768 Sun, Y.G., Wang, Q., Peng, L., Qi, Y.R., Bai, Y., 2020. Optimization on track vertical alignment of
769 subway lines with express/local trains. *J. Transp. Syst. Eng. Inf. Technol.* 20(4), 187–193.

770 Vandanjon, P.-O., Vinot, E., Cerezo, V., Coiret, A., Dauvergne, M., Bouteldja, M., 2019.
771 Longitudinal profile optimization for roads within an eco-design framework. *Transport. Res. Part*
772 *D: Transp. Environ.* 67, 642–658.

773 Wang, Q., Bai Y., Li J.J., Zhu Q.Z., Feng X.J., 2021. Optimization of station location and horizontal
774 alignment of underground urban rail transit. *J. Transp. Syst. Eng. Inf. Technol.* 21(2), 119–125.

775 Xin, T.Y et al., 2014. Railway vertical alignment optimisation at stations to minimise energy. 17th
776 *Inter. IEEE. Conf. on Intel. Transp. Sy. (ITSC).* 2119-2124. doi: 10.1109/ITSC.2014.6958016.

777 Zhang, H., Pu, H., Schonfeld, P., Song, T., Li, W., Hu, J., 2021. Railway alignment optimization
778 considering lifecycle costs. *IEEE. Intel. Transp. Sy.* 99, 2–20. doi:10.1109/MITS.2021.3071032.

779 Zhou Y., Bai Y., Li J.J., Mao B., Li T., 2018. Integrated optimization on train control and timetable

780 to minimize net energy consumption of metro lines. *J. Adv. Transp.* 2018, 1–19.